Supramolecular Microgels Fabricated from Supramonomers

Qiao Song,[†,‡] Yongfeng Gao,[§,‡] Jiang-Fei Xu,[†] Bo Qin,[†] Michael J. Serpe,[*,§] and Xi Zhang[*,†]

† The Key Lab of Organic Optoelectronics & Molecular Engineering, Department of Chemistry, Tsinghua University, Beijing 100084, China

§ Department of Chemistry, University of Alberta, Edmonton, Alberta, Canada

ABSTRACT: This letter describes a new method for fabricating supramolecular microgels from supramonomers. To this end, we designed and assembled supramonomers with one acrylate moiety on each end on the basis of noncovalent host-guest interactions, which could be utilized as a cross-linker. Then supramolecular microgels were fabricated through the copolymerization of supramonomers and *N*-isopropylacrylamide (NIPAm). The supramolecular microgels showed not only temperature-responsive properties as expected from conventional PNIPAm-based microgels, but also exhibited stimuli-responsive and degradable properties benefitting from the dynamic nature of supramonomers. In addition, it was found that the degradation kinetics of the supramolecular microgels was related greatly to the structure of the microgels, providing a way to tune the degradation kinetics of the supramolecular microgels. Various supramolecular microgels with desired structure and function are supposed to be facilely fabricated from supramonomers. It is anticipated that the supramolecular microgels can enrich the application of microgels by easily endowing the microgels with stimuli-responsive and degradable properties.

Supramonomers are bifunctional monomers that are generated via their noncovalent interaction with a chemical unit that holds them together, which can be utilized in the fabrication of supramolecular polymers.[1] Different from the traditional supramolecular polymerization,[2-14] supramonomers are first fabricated through noncovalent synthesis, and then supramolecular polymers are constructed through traditional (covalent) polymerization of the supramonomers. In the past few years, efforts have been made for the synthesis of supramolecular polymers from various types of supramonomers through different polymerization methods, demonstrating its general applicability in the fabrication of supramolecular polymers.[15-20] Meanwhile, it is of significant importance to employ the dynamic nature of supramonomers for the fabrication of functional supramolecular materials.

Poly-(*N*-isopropylacrylamide) (PNIPAm)-based microgels are well-known temperature responsive (i.e., thermoresponsive) materials that can be used for a variety of applications.[21-28] For example, they have been used for sensing,[29-34] chemical separation,[35] drug delivery,[36-38] and artificial muscles.[39-41] PNIPAm-based microgels are typically synthesized by copolymerizing NIPAm with various functional monomers using *N*,*N*'-methylenebis(acrylamide) (BIS) as cross-linker in aqueous solution. Microgels fabricated in this way are of thermoresponsivity, however with BIS as cross-linker, the covalently cross-linked microgels are undegradable, which might limit their use in certain conditions, such as biological and environmental.

In this letter, supramonomers were used as a supramolecular cross-linker to fabricate supramolecular microgels. The dynamic nature of supramonomers may endow the supramolecular microgels with stimuli-responsive and degradable properties. As shown in Scheme 1, we first designed and synthesized a guest molecule, Phe-Gly-Gly linked with an acrylate moiety via esterification reaction (FGG-EA). Based on the specific host-guest supramolecular complexation, the tripeptide derivative FGG-EA was allowed to complex with cucurbit[8]uril (CB[8]) in a molar ratio of 2:1 to give supramonomers with one acrylate moiety at each end.[42-47] Then the supramonomers were used as a supramolecular cross-linker to copolymerize with NIPAm in aqueous solution, obtaining supramolecular microgels, which we hypothesize will exhibit both the thermoresponsivity of the PNIPAm-based microgels and degradable properties attributed to the supramonomers. The concept of supramonomers provides us a facile strategy towards the fabrication of supramolecular microgels, which may greatly enrich the application of microgels.

Scheme 1. Fabrication of supramolecular microgels from supramonomers.

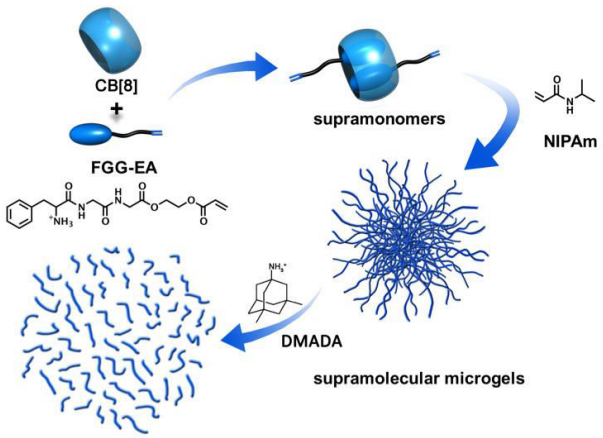

The supramonomers were prepared by simply mixing FGG-EA and CB[8] in a molar ratio of 2:1 in aqueous solution. The formation of supramonomers was studied by ^{1}H NMR. As shown in Figure 1a, peaks at ~7.25 ascribed to the aromatic ring of FGG shifted to higher field after the complexation of FGG with CB[8] while no residual signals from free FGG were detected, indicating that FGG-EA and CB[8] formed a complex and the binding ratio should be 2:1. The ESI-MS data showed a molecular ion peak with a mass/charge ratio of 1042.36, which is in good accordance with the calculated molecular weight of the supramonomer with two positive charges (Figure S2). Moreover, ITC results further confirmed the formation of supramonomers. As shown in Figure 1b, there was an abrupt transition at molar ratio of 2.0. By fitting the titration curve, the binding constant can be calculated to be 2.0×10^{11} M^{-2}. Therefore, the high binding affinity guarantees the formation of supramonomers with well-defined composition.

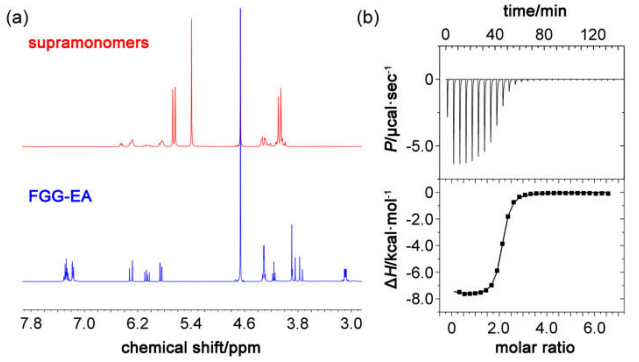

Figure 1. (a) Partial ^{1}H NMR spectra of supramonomers and FGG-EA. (b) ITC data for titration of CB[8] (0.1 mM) with FGG-EA (2.0 mM) in 50 mM NaAc/HAc buffer (pH = 4.7) at 25 °C. Fitting data using two sets of the binding site model gave a binding constant of 2.0×10^{11} M^{-2}.

Supramolecular microgels were then synthesized through the copolymerization of NIPAm and supramonomers with the supramonomer molar percentage of 5%. As shown in the transmission electron microscope (TEM) images, spherical microgels with diameter around 400 nm were observed in the dry state (Figure 2a). Furthermore, DLS gave detailed size information about the microgels (Figure 2b). The hydrated diameter of the microgels was ~900 nm at 25 °C, which decreased to ~550 nm at 45 °C, demonstrating the thermoresponsivity. The lower critical solution temperature (LCST) of the microgels was measured based on turbidimetric analysis attributed to light scattering. The absorbance (i.e., scattering) of the microgel aqueous dispersions was investigated by measuring UV/vis spectra at various temperatures. By plotting the absorbance at 250 nm against temperature, as shown in Figure 2c, the LCST of microgels is around 37 °C. In addition, we cycled the temperature between 25 °C and 45 °C over many times. The size of the supramolecular microgels was consistent from cycle to cycle (Figure S3), showing good reversibility and stability, which guarantees its practical application as conventional PNIPAm-based microgels.

To confirm that the supramonomers did act as a cross-linker during the formation of supramolecular microgels, ^{1}H NMR spectrum of microgels was conducted (Figure S4). Microgels showed broad signals due to their large aggregates, and peaks ascribed to CB[8] could be observed. At the same time, no peaks belonging to the double bonds of free supramonomers were detected. Moreover, by integrating peaks ascribed to supramonomer and PNIPAm, the molar percentage of the supramonomer was calculated to be 5.4%, which was close to the initial ratio used for the supramolecular microgel fabrication.

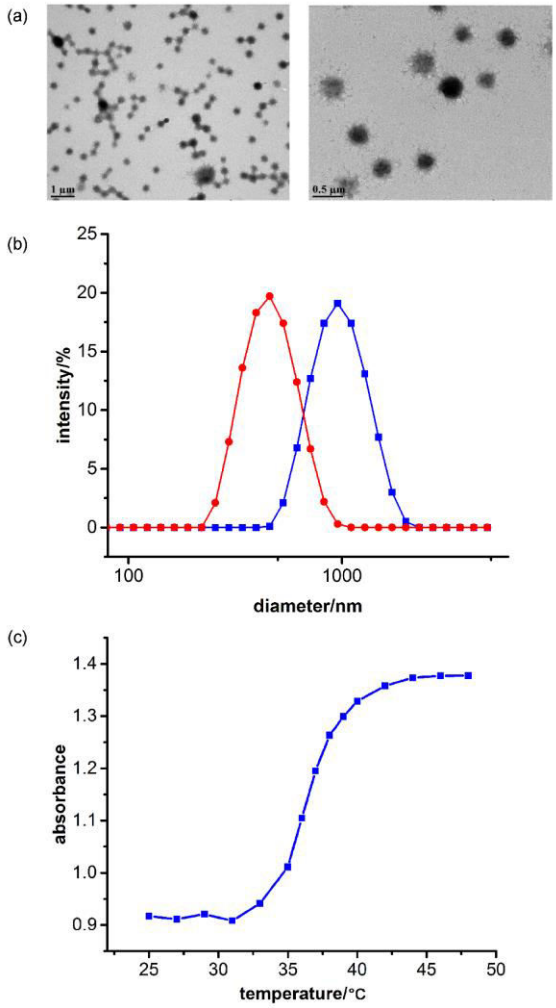

Figure 2. (a) TEM images of supramolecular microgels. (b) DLS data of supramolecular microgels at (blue, squares) 25 °C and (red, circles) 45 °C. (c) LCST of supramolecular microgels monitored by UV/vis spectroscopy.

Benefitting from the dynamic nature of the supramonomers, the microgels can undergo degradation when exposed to certain stimuli. 3,5-Dimethyl-1-adamantanamine hydrochloride (DMADA), which has a much higher binding constant with CB[8] (4.33×10^{11} M^{-1}) than FGG-EA,[48] can be utilized as chemical stimuli to destroy the supramonomers. When adding equimolar amount of DMADA into the solution of supramonomers, as revealed by ^{1}H NMR spectra (Figure S6), peaks belonging to FGG-EA shifted back, suggesting the disassociation of the supramonomers. As shown in Figure 3a, upon adding DMADA into the aqueous solution of microgels, the translucent solution became transparent, suggesting that the microgels were thoroughly degraded. It is also possible to monitor the degradation process *in situ* via microscopy (Figure 3c). After dripping one droplet of the microgel aqueous dispersion onto the microscope slide, microgels were found in both water phase and dry phase after water evaporation. How-

ever, after adding DMADA into the microgel drop on the slide *in situ*, microgels in the water phase vanished while microgels in the dry phase remained unchanged. As indicated by DLS (Figure 3b), after adding DMADA, only small aggregates with diameter below 100 nm were detected, supporting the degradation of microgels. In the meantime, conventional microgels using BIS as cross-linker were prepared as control. DLS showed no clear change upon adding DMADA (Figure S7).

We also wanted to determine if the microgel degradation process could be attributed to the disassociation of the supramonomers. To answer this question, ^{1}H NMR spectrum of microgels after adding DMADA was conducted. As shown in Figure S8, peaks ascribed to CB[8] were found to become much sharper than that of the microgels, suggesting the disappearance of large aggregates. In the meantime, peaks at ~7.3 ppm could be assigned to free FGG moieties, also indicating the specific noncovalent interactions between FGG and CB[8] were disrupted. Therefore, it is the DMADA that causes the disassociation of the supramonomers, followed by the degradation of the microgels.

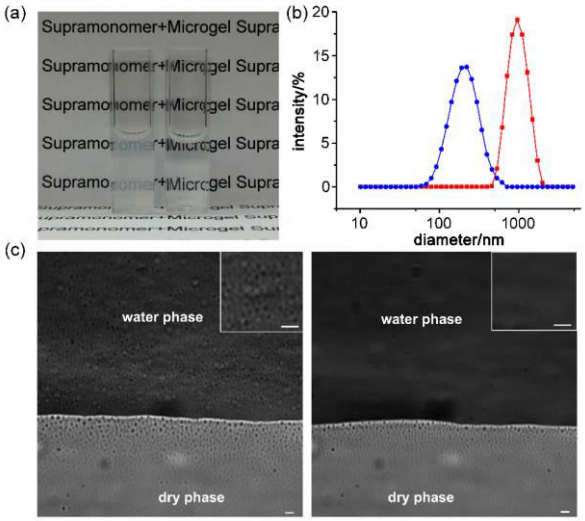

Figure 3. (a) Photo of supramolecular microgels before (left) and after (right) adding DMADA. (b) DLS data of supramolecular microgels before (red) and after (blue) adding DMADA. (c) Microscopic images of supramolecular microgels before (left) and after (right) adding DMADA (Scale bar: 4 μm).

Moreover, the degradation kinetics of the microgels can also be revealed by UV/vis spectroscopy. By monitoring the change of absorbance at 260 nm against time after the addition of DMADA, the relationship between microgel degradation ratio and degradation time could be obtained (Figure S9). Simulated according to the principle of first-order reaction, the degradation rate constant is about 2.96×10^{-3} s^{-1}. It should be noted that the degradation rate constant in microgels is much smaller than the dissociation rate of CB[8]-related association and disassociation. Therefore, the slow diffusion of DMADA into the microgels could be responsible for the low degradation rate.

It is assumed that the degradation kinetics relates greatly to the structure of the microgels. As is known, the thermoresponsive microgels tend to expel their water of solvation and deswell when heated above LCST and reswell when cooled below LCST. Below LCST, the microgels exhibit fully swelled structure, making the relatively small molecule DMADA easy to diffuse in. However, above LCST, the microgels exhibit dense and collapsed structure, making the DMADA molecule hard to diffuse in. In other words, the degradation kinetics should be quite different below and above LCST. In this regard, the degradation kinetics at different temperatures was investigated. According to the degradation rate constant at different temperatures, the apparent activation energy (E_a) as well as preexponential factor (A) below LCST (15.0 °C, 17.5 °C, 20.0 °C, 22.5 °C, 25.0 °C) and above LCST (45.0 °C, 47.5 °C, 50.0 °C, 52.5 °C, 55.0 °C) could be calculated based on Arrhenius formula, respectively, as shown in Figure 4. The preexponential factor A above LCST ($A = 1.79 \times 10^6$ s^{-1}) is much smaller than that below LCST ($A = 9.80 \times 10^7$ s^{-1}), indicating that it is much more difficult for DMADA to diffuse into the microgels above LCST. In the meantime, the apparent activation energy E_a above LCST (E_a = 52.7 kJ/mol) is slightly smaller than that below LCST (E_a = 59.9 kJ/mol), which could be attributed to the relatively higher local CB[8] concentration in the microgels above LCST, making it easier for DMADA to destroy the crosslinking points once it has already diffused into the microgels. To further confirm the influence of microgel structure on the degradation kinetics, degradation process upon time at 35 °C and 38 °C was studied and compared. As shown in Figure S10, the degradation is much faster at 35 °C (swelled structure) than 38 °C (collapsed structure), proving that the degradation kinetics are closely related to the microgel structure. Therefore, this study provides a facile way to tune the degradation kinetics of the supramolecular microgels.

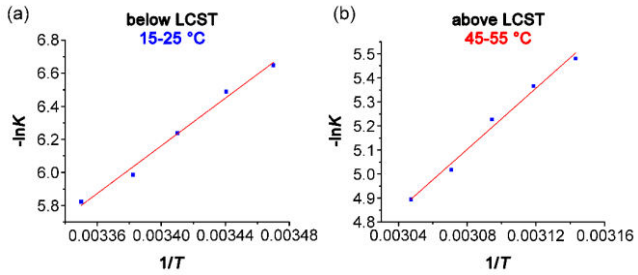

Figure 4. Fitting of degradation rate constant (K) to degradation temperature (T) based on Arrhenius Equation to give the apparent activation energy (E_a) and preexponential factor (A) below LCST (a) and above LCST (b).

It should be pointed out that the supramolecular microgels can undergo degradation under various stimuli. For example, triethylamine (TEA) can destroy the multiple hydrogen bonding between FGG-EA and CB[8], leading to the disassociation of the supramonomers, thus causing the degradation of the microgels, which could be proved by DLS as well as naked eye (Figure S11).

In conclusion, for the first time we have employed the concept of supramonomers for the fabrication of supramolecular microgels. The supramolecular microgels exhibit not only thermal responsive properties as conventional microgels but also dynamic and degradable properties due to the introduction of supramonomers. In principle, supramonomers with various architectures can be constructed on the basis of different noncovalent interactions. Different monomers could be used to copolymerize with supramonomers to form supramolecular microgels. Therefore, it is highly anticipated that the similar

strategy can be extended to fabricate various supramolecular microgels with tailor-made structure and function.

ASSOCIATED CONTENT

Supporting Information

The Supporting Information is available free of charge on the ACS Publications website.

Synthesis of compounds, methods, NMR spectra, DLS data and degradation kinetics (PDF)

AUTHOR INFORMATION

Corresponding Author

* E-mail: xi@mail.tsinghua.edu.cn.
* E-mail: michael.serpe@ualberta.ca.

Author Contributions

‡These authors contributed equally.

Notes

The authors declare no competing financial interest.

ACKNOWLEDGMENT

This work was financially supported by the National Natural Science Foundation of China (21434004, 21274076), the NSFC Innovation Group (21421064) and NSERC.

REFERENCES

(1) Yang, L.; Liu, X.; Tan, X.; Yang, H.; Wang, Z.; Zhang, X. *Polym. Chem.* **2014**, *5*, 323.

(2) Yang, L.; Tan, X.; Wang, Z.; Zhang, X. *Chem. Rev.* **2015**, *115*, 7196.

(3) Fouquey, C.; Lehn, J.-M.; Levelut, A.-M. *Adv. Mater.* **1990**, *2*, 254.

(4) Brunsveld, L.; Folmer, B. J. B.; Meijer, E. W.; Sijbesma, R. P. *Chem. Rev.* **2001**, *101*, 4071.

(5) De Greef, T. F. A.; Smulders, M. M. J.; Wolffs, M.; Schenning, A. P. H. J.; Sijbesma, R. P.; Meijer, E. W. *Chem. Rev.* **2009**, *109*, 5687.

(6) Yan, X.; Wang, F.; Zheng, B.; Huang, F. *Chem. Soc. Rev.* **2012**, *41*, 6042.

(7) Barrow, S. J.; Kasera, S.; Rowland, M. J.; del Barrio, J.; Scherman, O. A. *Chem. Rev.* **2015**, *115*, 12320.

(8) Liu, Y.; Yu, Y.; Gao, J.; Wang, Z.; Zhang, X. *Angew. Chem., Int. Ed.* **2010**, *49*, 6576.

(9) Liu, Y.; Liu, K.; Wang, Z.; Zhang, X. *Chem. - Eur. J.* **2011**, *17*, 9930.

(10) Huang, Z.; Yang, L.; Liu, Y.; Wang, Z.; Scherman, O. A.; Zhang, X. *Angew. Chem., Int. Ed.* **2014**, 53, 5351.

(11) Yang, L.; Bai, Y.; Tan, X.; Wang, Z.; Zhang, X. *ACS Macro Lett.* **2015**, *4*, 611.

(12) Xu, J.-F.; Huang, Z.; Chen, L.; Qin, B.; Song, Q.; Wang, Z.; Zhang, X. *ACS Macro Lett.* **2015**, *4*, 1410.

(13) Wei, P.; Yan, X.; Cook, T. R.; Ji, X.; Stang, P. J.; Huang, F. *ACS Macro Lett.* **2016**, 5, 671.

(14) Rui, L.; Liu, L.; Wang, Y.; Gao, Y.; Zhang, W. *ACS Macro Lett.* **2016**, *5*, 112.

(15) Roy, N.; Buhler, E.; Lehn, J.-M. *Polym. Chem.* **2013**, *4*, 2949.

(16) Xu, J.-F.; Chen, Y.-Z.; Wu, L.-Z.; Tung, C.-H.; Yang, Q.-Z. *Org. Lett.* **2013**, *15*, 6148.

(17) Song, Q.; Li, F.; Tan, X.; Yang, L.; Wang, Z.; Zhang, X. *Polym. Chem.* **2014**, *5*, 5895.

(18) Song, Q.; Li, F.; Yang, L.; Wang, Z.; Zhang, X. *Polym. Chem.* **2015**, *6*, 369.

(19) Huang, Z.; Fang, Y.; Luo, Q.; Liu, S.; An, G.; Hou, C.; Lang, C.; Xu, J.; Dong, Z.; Liu, J. *Chem. Commun.* **2016**, *52*, 2083.

(20) Liu, X.; Xu, J.-F.; Wang, Z.; Zhang, X. *Polym. Chem.* **2016**, *7*, 2333.

(21) Pelton, R. H.; Chibante, P. *Colloids Surf.* **1986**, *20*, 247.

(22) Pelton, R. *Adv. Colloid Interface Sci.* **2000**, *85*, 1.

(23) Ballauff, M.; Lu, Y. *Polymer* **2007**, *48*, 1815.

(24) Lyon, L. A.; Meng, Z.; Singh, N.; Sorrell, C. D.; St. John, A. *Chem. Soc. Rev.* **2009**, *38*, 865.

(25) Zhang, Q. M.; Xu, W.; Serpe, M. J. *Angew. Chem., Int. Ed.* **2014**, *53*, 4827.

(26) Hoare, T.; Pelton, R. *Macromolecules* **2004**, *37*, 2544.

(27) Zhang, W.; Zhang, W.; Cheng, Z.; Zhou, N.; Zhu, J.; Zhang, Z.; Chen, G.; Zhu, X. *Macromolecules* **2011**, 44, 3366.

(28) Sun, S.; Wu, P.; Zhang, W.; Zhang, W.; Zhu, X. *Soft Matter* **2013**, 9, 1807.

(29) Sorrell, C. D.; Serpe, M. J. *Adv. Mater.* **2011**, *23*, 4088.

(30) Liu, T.; Hu, J.; Yin, J.; Zhang, Y.; Li, C.; Liu, S. *Chem. Mater.* **2009**, *21*, 3439.

(31) Gao, Y.; Li, X.; Serpe, M. J. *RSC Advances* **2015**, 5, 44074.

(32) Li, X.; Gao, Y.; Serpe, M. J. *Macromol. Rapid Commun.* **2015**, *36*, 1382.

(33) Zheng, X.; Qian, J.; Tang, F.; Wang, Z.; Cao, C.; Zhong, K. *ACS Macro Lett.* **2015**, *4*, 431.

(34) Yuan, Q.; Gu, J.; Zhao, Y.-n.; Yao, L.; Guan, Y.; Zhang, Y. *ACS Macro Lett.* **2016**, 5, 565.

(35) Parasuraman, D.; Serpe, M. J. *ACS Appl. Mater. Interfaces* **2011**, *3*, 4714.

(36) Oh, J. K.; Drumright, R.; Siegwart, D. J.; Matyjaszewski, K. *Prog. Polym. Sci.* **2008**, *33*, 448.

(37) Guan, Y.; Zhang, Y. *Soft Matter* **2011**, *7*, 6375.

(38) Gao, Y.; Zago, G. P.; Jia, Z.; Serpe, M. J. *ACS Appl. Mater. Interfaces* **2013**, *5*, 9803.

(39) Islam, M. R.; Li, X.; Smyth, K.; Serpe, M. J. *Angew. Chem., Int. Ed.* **2013**, 52, 10330.

(40) Li, X.; Serpe, M. J. *Adv. Funct. Mater.* **2014**, *24*, 4119.

(41) Li, X.; Serpe, M. J. *Adv. Funct. Mater.* **2016**, *26*, 3282.

(42) Heitmann, L. M.; Taylor, A. B.; Hart, P. J.; Urbach, A. R. *J. Am. Chem. Soc.* **2006**, *128*, 12574.

(43) Nguyen, H. D.; Dang, D. T.; van Dongen, J. L. J.; Brunsveld, L. *Angew. Chem., Int. Ed.* **2010**, *49*, 895.

(44) Dang, D. T.; Schill, J.; Brunsveld, L. *Chem. Sci.* **2012**, *3*, 2679.

(45) Hou, C.; Li, J.; Zhao, L.; Zhang, W.; Luo, Q.; Dong, Z.; Xu, J.; Liu, J. *Angew. Chem., Int. Ed.* **2013**, *52*, 5590.

(46) Tan, X.; Yang, L.; Liu, Y.; Huang, Z.; Yang, H.; Wang, Z.; Zhang, X. *Polym. Chem.* **2013**, *4*, 5378.

(47) Ramaekers, M.; Wijnands, S. P. W.; van Dongen, J. L. J.; Brunsveld, L.; Dankers, P. Y. W. *Chem. Commun.* **2015**, *51*, 3147.

(48) Liu, S.; Ruspic, C.; Mukhopadhyay, P.; Chakrabarti, S.; Zavalij, P. Y.; Isaacs, L. *J. Am. Chem. Soc.* **2005**, *127*, 15959.

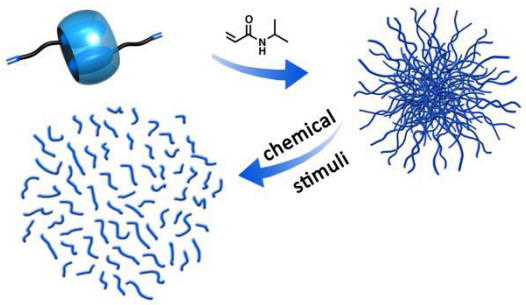
chemical
stimuli